Metal-Organic Frameworks

Overcoming Crystallinity Limitations of Aluminium Metal-Organic Frameworks by Oxalic Acid Modulated Synthesis**

Stefano Canossa[+],*[a, c] Adrian Gonzalez-Nelson[+],[a, b] Leonid Shupletsov,[a] Maria del Carmen Martin,[a] and Monique A. Van der Veen*[a]

Abstract: A modulated synthesis approach based on the chelating properties of oxalic acid ($H_2C_2O_4$) is presented as a robust and versatile method to achieve highly crystalline Al-based metal-organic frameworks. A comparative study on this method and the already established modulation by hydrofluoric acid was conducted using MIL-53 as test system. The superior performance of oxalic acid modulation in terms of crystallinity and absence of undesired impurities is explained by assessing the coordination modes of the two modulators and the structural features of the product. The validity of our approach was confirmed for a diverse set of Al-MOFs, namely X-MIL-53 (X = OH, CH_3O, Br, NO_2), CAU-10, MIL-69, and Al(OH)ndc (ndc = 1,4-naphtalenedicarboxylate), highlighting the potential benefits of extending the use of this modulator to other coordination materials.

Introduction

Among porous materials, metal-organic frameworks (MOFs) stand out for the extraordinary diversity of their applications. Such versatility arises from the combined use of a virtually endless variety of inorganic and organic building units (known as IBUs and linkers, respectively). Although this hybrid structure can endow MOFs with an outstanding number of functionalities, it also limits their chemical and thermal stabilities, which are substantially lower compared to already established porous inorganic materials such as zeolites[1–3] and porous metal oxides.[4] For this reason, the research of stable MOFs is of utmost importance to guarantee long-term unaltered performance, especially for applications involving non-standard conditions such as catalysis or gas separation. In this regard, Al-MOFs are of special interest as they combine high operating temperatures,[5] convenient syntheses in aqueous media,[6–8] and high natural abundance of the metal sources. Moreover, their exceptional chemical stability[9,10] in both aqueous and organic media makes this class of materials ideal for applications that are unsuitable for most MOFs, such as moisture harvesting,[11,12] adsorption-driven heat exchange,[13–15] and water remediation.[16] Unfortunately, the synthesis of highly crystalline Al-MOFs is a long-standing challenge as most of these can only be obtained as nanocrystalline powders[9,17,18] and such limitations are known to have detrimental effects on MOFs' porosity and sorption capacity.[19–21] Importantly, increasing the achievable crystal size of MOFs enables the detailed description of their structural features by single-crystal X-ray diffraction (SCXRD) and the investigation of functional properties of interest, such as mechanical response[22–25] and electronic behavior.[26–28] Monocarboxylate modulators, commonly used in MOF synthesis, have shown to lead to defect formation[29] and even decrease in crystal size.[30] To date, the only effective approach that has been reported for the synthesis of highly crystalline Al-MOFs is based on the use of hydrofluoric acid,[31–34] borrowing from its well-documented use as mineralizer to improve the crystallinity of microporous inorganic materials.[35] Its widespread use, however, raises concerns both on safety and on the possible fluoride inclusion in the framework architecture.

In this context, we present here a versatile and efficient modulated synthesis approach able to improve substantially the crystallinity of Al-MOFs while maintaining their structure and composition unaltered. Our method is based on the use of a natural and abundant molecule: oxalic acid (chemical for-

[a] Dr. S. Canossa,[+] A. Gonzalez-Nelson,[+] L. Shupletsov, M. del Carmen Martin, Dr. M. A. Van der Veen
Department of Chemical Engineering
Delft University of Technology
Van der Maasweg 9, 2628 BZ Delft (The Netherlands)
E-mail: stefano.canossa@uantwerpen.be
m.a.vanderveen@tudelft.nl

[b] A. Gonzalez-Nelson[+]
DPI, P.O.Box 92
5600 AX Eindhoven (The Netherlands)

[c] Dr. S. Canossa[+]
Current affiliation: EMAT, Department of Physics
University of Antwerp, Groenenborgenlaan 171
2020 Antwerp (Belgium)

[+] These authors contributed equally.

[**] A previous version of this manuscript has been deposited on a preprint server (https://doi.org/10.26434/chemrxiv.9999572.v1).

Supporting information and the ORCID identification number(s) for the author(s) of this article can be found under: https://doi.org/10.1002/chem.201904798.

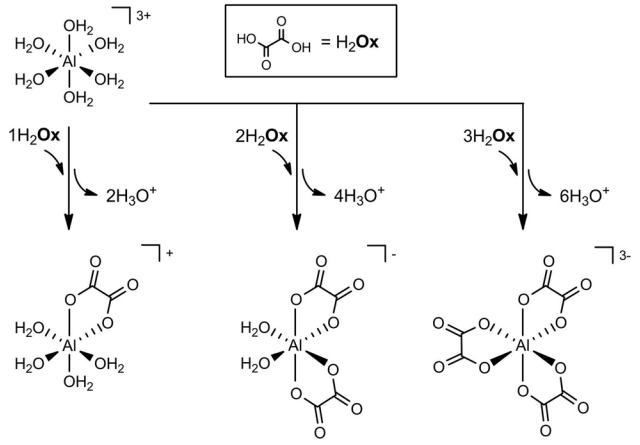

Scheme 1. The possible hetero- and homoleptic complexes formed in water by Al^{3+} and oxalic acid.

mula: $H_2C_2O_4$; Scheme 1). Although the high stability of its hetero- and homoleptic aluminium complexes has long been known in environmental and geological sciences,[36,37] its potential as synthesis modulator has never been studied.

Results and Discussion

We first tested the effects of this molecule in the synthesis of the widely researched MIL-53(Al)[38] (chemical formula Al(OH)bdc; bdc = 1,4-benzendicarboxylate) and compared its efficacy, under equal synthetic conditions, with those of other modulators, namely HCl, HF, NH_4F, and sodium oxalate. This choice allowed us to decouple the effects of acidity and coordination modulation and to evaluate the advantages of our approach over the already established use of HF. Whereas the increase of H_3O^+ concentration has positive effects on the crystallinity in general, the 10 μm average crystal size observed by using HCl increases 4-fold with HF and 8-fold with oxalic acid (Figure 1a, Figures S3–S8), suggesting that the anion's coordinative capabilities have the most significant influence. However, in the case of fluoride modulation, the crystal size was not the only observed change as X-ray powder diffraction (XRPD) patterns show the presence of a secondary phase (Figure 1b). This is supported by the appearance of a secondary combustion process in the thermogravimetric profiles (Figure S37). These differences agree with the formation of a fluorine-substituted form of MIL-53, Al(F)bdc, whose properties differ significantly from those of the fluorine-free material, especially concerning its renowned breathing behavior.[39]

This compound, first reported by Liu et al,[40] has also been observed as impurity in a recent paper on the use of HF to increase the crystallinity of MIL-53.[32] Energy dispersive X-ray spectroscopy (EDX) analysis on rinsed product obtained by HF-modulated synthesis shows that all the observed crystals are contaminated with fluoride inclusions (Figures 1c and S36). This evidence indicates that Al(F)bdc is present as crystalline domains within MIL-53 crystals rather than as a pure phase. This is further corroborated by the absence of structured diffuse scattering in high-resolution SCXRD data from contaminated crystals (Figures S54–S55).[41,42] Additionally, a minor fraction of the crystals exhibit a higher density of aluminium and fluorine, in line with the previously reported presence of undesired AlF_3 (Figure 1c, Figure S36, and Table S3).[33] Considering all the evidence, it can be concluded that the use of fluoride modulation in MIL-53 synthesis yields crystals with inclusions of Al(F)bdc, and AlF_3 as by-product.

The oxalate-modulated syntheses, on the other hand, yielded pure MIL-53 crystals as evidenced by XRPD analysis (Fig-

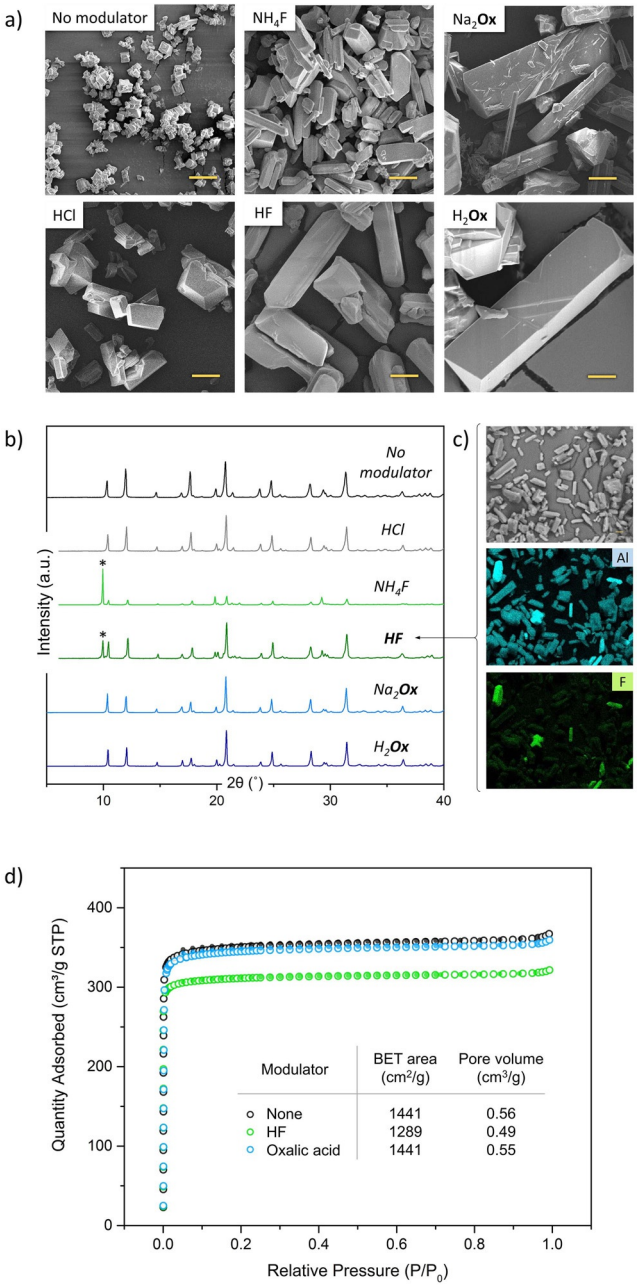

Figure 1. (a) SEM images of MIL-53 crystals obtained by normal and modulated syntheses (scale bar = 10 μm). XRPD (b) and EDX analysis (c) show the presence of Al(F)bdc (marked *) and AlF_3 when a fluoride-based modulator is used. (d) N_2 adsorption (empty circles) and desorption (filled circles) isotherms showing a decrease of BET area and pore volume for HF-modulated MIL-53.

ure 1 b). Their thermogravimetric profiles show no sign of oxalate species in the framework or missing linker defects (Figure S37). Moreover, nitrogen sorption measurements show no substantial difference, in terms of BET surface area and pore volume, between the unmodulated and the oxalic acid-modulated products (Figure 1 d). By comparison, the products obtained by using HF show instead a loss of BET area and pore volume of approximately 10%. Since this difference is mainly attributable to the presence of impurities of non-porous AlF_3 in the sample (ca. 4.5% w/w calculated from the TGA profile), it is not possible to assess with precision the effects of the fluoride inclusions in the MIL-53 framework based on the sorption behavior. Nevertheless, these results further demonstrate the detrimental effects of fluoride-based synthesis modulation and the capability of oxalic acid to increase the MOF's crystallinity without causing compositional modifications.

The main reason for these effects can be found in the characteristic κ^2 chelation mode of oxalic acid and the high stability of the resulting five-membered ring (Scheme 2 a). The participation of oxalate in the framework would require it either to adopt a poorly stable μ_2-1,3 coordination using only one of its carboxylate groups or to bridge the aluminium centers using both groups (i.e., μ_2-1,4 bridging), which is incompatible with the MIL-53 structure both in terms of charge and IBU coordination geometry. This is further supported by the absence of both types of oxalate-aluminium coordination geometries in the CSD database (see Supporting Information, page 27).[43]

On the contrary, fluoride coordination to aluminium is fully compatible with the substitution of hydroxy groups in the framework since both anions are monodentate, have analogous size, and feature same charge and number of valence electron pairs (Scheme 2 b). For similar reasons, until now the use of short-chain monocarboxylic acids as synthesis modulators for Al-MIL-53 as well as for other Al-MOFs focused on taking advantage of their tendency for linker replacement[44] to hamper the growth of specific crystal facets,[45,46] reduce the mean crystal size,[30] and introduce structural defects to modify the MOF's porosity.[29,47]

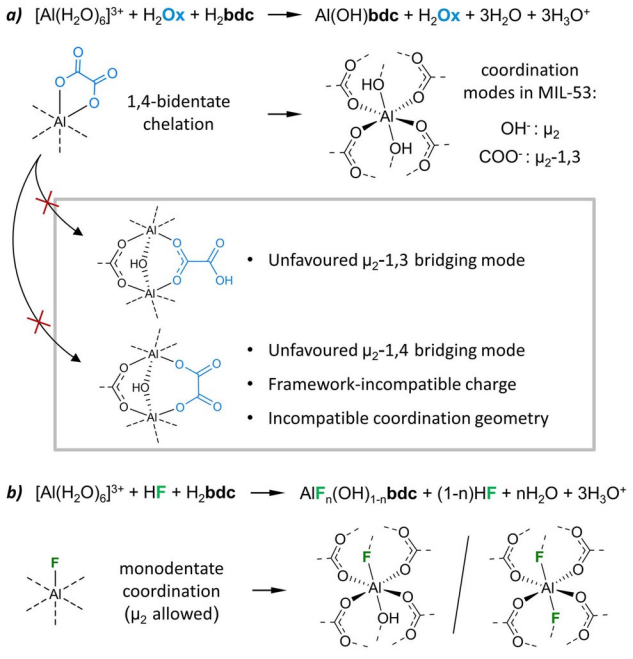

Scheme 2. The reaction formulas for MIL-53 synthesis modulated by oxalic acid (a) and hydrofluoric acid (b).

The benefits of oxalic acid modulation are not limited to MIL-53, as they were also observed for its analogues with OH-, CH_3O-, Br-, and NO_2-functionalised linkers. These MOFs were synthesized using 0.5, 1, and 1.5 oxalic acid:Al ratios to study how the amount of modulator affects the crystallinity of the products. In all the studied systems, oxalic acid leads to an increased crystal size with respect to the unmodulated synthesis (Figure 2, Figures S9–S23). Interestingly, a higher modulator-to-Al ratio does not always result in improved crystallinity. Indeed, in the cases of OH- and CH_3O-MIL-53, an excessive amount of modulator leads to the stabilization of a specific size or the absence of solid products, respectively. This behavior can be attributed to the electron-donor character of OH and CH_3O groups,[48] which lowers the acidity of terephthalic acid by destabilizing its conjugated base.[49] Additionally, the pH decrease due to the MOF synthesis and to the formation of aluminium oxalate complexes further disfavors the deprotonation of the linkers, thus diminishing their reactivity. Our results show that the combination of these effects can allow for the tuning of the product's size distribution, in addition to its crystallinity. However, to achieve such control, several aspects should be considered, in particular the modulator concentration, the species formed during the synthesis, and the chemical properties of the linker. Therefore, the adequate conditions to stabilize a specific size must be optimized for every system.

A peculiar behavior is observed for NO_2-MIL-53, whose crystal quality improves with the use of modulator but drops significantly when a modulator:Al ratio of 1.5 is used. The XRPD patterns of all NO_2-MIL-53 products (Figure S48) show broad diffuse scattering bands, also observed by SCXRD (Figure S56). These signals are attributable to a local ordering of the NO_2 groups, which can be found disordered in four equivalent positions for every linker after the MOF assembly. The effect of the modulator in slowing the crystal growth can favor this ordering and allow the formation of larger ordered domains, which could grow clustered in polycrystalline aggregates like those observed by SEM for the products obtained with the highest modulator concentration. Further experiments to confirm this hypothesis and determine the ordering of the NO_2 groups will be the focus of our future research.

Having confirmed the effectiveness of oxalic acid in the synthesis of functionalized MIL-53, we extended its use to additional Al-MOFs with varying linker molecules and IBUs, namely CAU-10,[50] MIL-69,[51] and Al(OH)ndc[52] (ndc = 1,4-naphtalenedicarboxylate). These three materials were obtained as nanocrystalline powders by conventional synthesis, whereas the introduction of oxalic acid modulation afforded crystals up to 5 μm for CAU-10, 20 μm for MIL-69, and 70 μm for Al(OH)ndc (Figure 2, Figures S24–S35). Although the performance of the modulator depends strongly on the type of material, the oxalic acid modulation method proved its validity on these systems

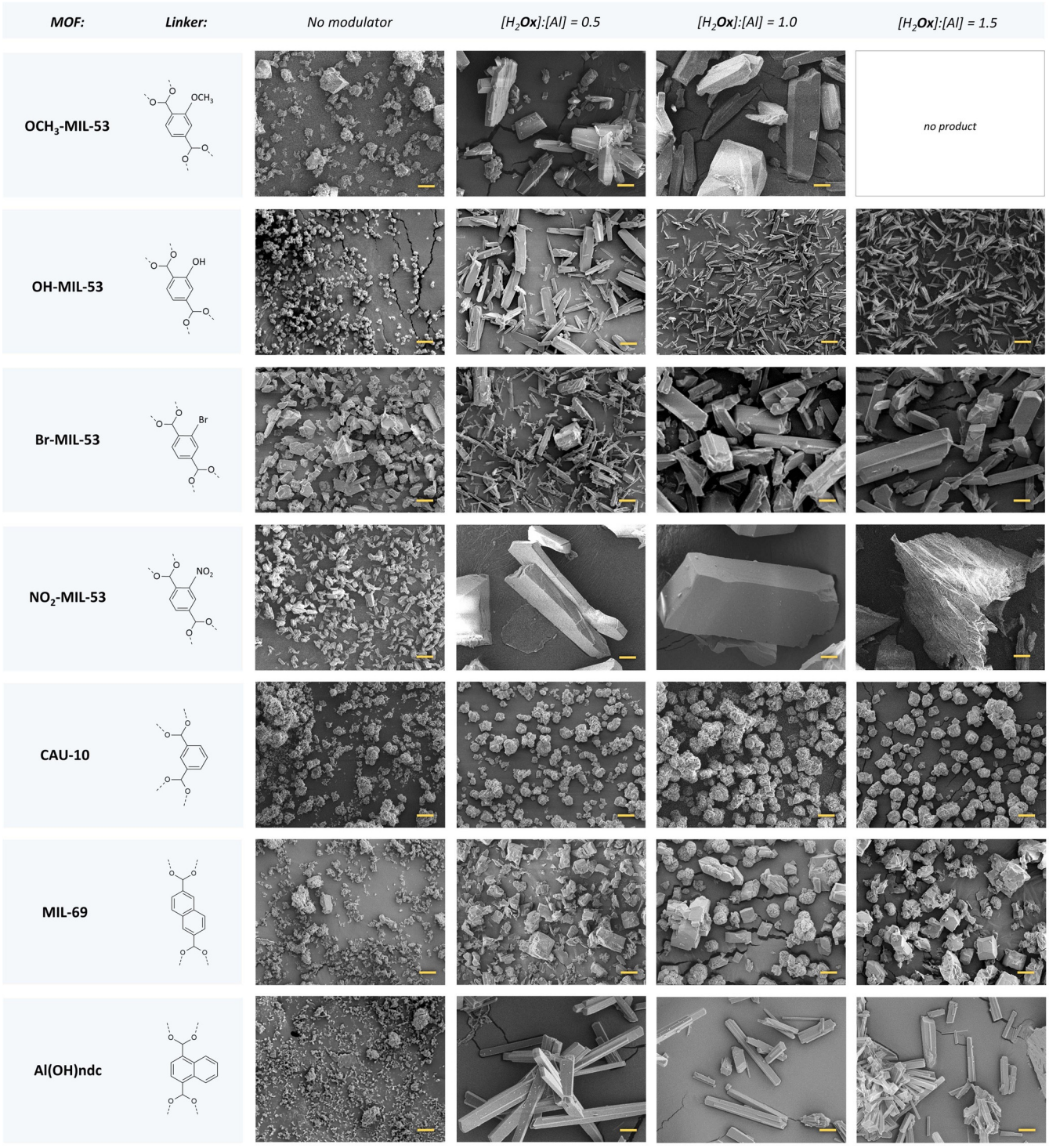

Figure 2. SEM images of functionalized MIL-53, CAU-10, MIL-69 and Al(OH)ndc crystals synthesized without modulator and with different modulator concentrations (scale bar = 10 μm).

despite their different structure and assembly. Even in the case of the notably different linker geometry and IBU structure of CAU-10, the kinetic control introduced by oxalic acid coordination to the metals improves the crystallinity while limiting the occurrence of crystal twinning and the formation of intergrown domains.

Conclusions

The use of oxalic acid as synthesis modulator for various Al-MOFs affords products with an unprecedented crystallinity without affecting the materials' structure and composition. Although the outcome of this approach is highly dependent on

the framework's structure as well as on the synthetic conditions, its efficacy has been confirmed for all the examined systems regardless of linker functionalization or type of material. We attribute this remarkable versatility to oxalic acid's synergistic action in both binding the metals and protonating the linkers, thus introducing a substantial control over the MOF nucleation and regulating the crystal growth. Furthermore, we described how the strong differences between its characteristic five-membered ring chelation and the linker's coordination mode in the studied materials allow the modulating function without causing substitutional defects. These advantages do not apply in the case of modulators whose coordination capabilities are compatible with those found in the IBUs, such as fluoride or monocarboxylate species. Further applications of oxalic acid modulation to other Al-MOFs, as well as frameworks based on different metals, will be crucial to assess more thoroughly its validity and highlight additional MOF-specific particularities and advantages associated with its use.

Experimental Section

Reagents and solvents: All solvents and reagents, except for 2-methoxyterephtalic acid and anhydrous sodium oxalate, were purchased by commercial suppliers and used as-received. A complete list including purity and suppliers can be found in the Supporting Information.

Synthesis of 2-methoxyterephtalic acid: 2-Methoxyterephthalic acid was synthesized according to a reported method.[53] A mixture of 2,5-dimethylanisole (7.76 g, 57 mmol), $KMnO_4$ (25.0 g, 158 mmol), and NaOH (3.10 g, 77.5 mmol) in water (500 mL) was heated to 60 °C. After 5 h, an additional amount of $KMnO_4$ (25.0 g, 158 mmol) was added, and refluxed for 1 h. The mixture was cooled to room temperature and filtered over paper. The filtrate was acidified with conc. HCl (37%), and the resulting white precipitate was collected by filtration and dried under vacuum at 60 °C for 12 h. Yield: 4.5 g, 40%. ^{1}H NMR (400 MHz, [D$_6$]DMSO) δ 13.12 (br. s, 2H, COOH), 7.68 (d, J = 7.8 Hz, 1H, $C_{Ar}H$), 7.57 (d, J = 1.4 Hz, 1H, $C_{Ar}H$), 7.55 (dd, J = 7.8, 1.4 Hz, 1H, $C_{Ar}H$), 3.87 (s, 3H, CH_3), Figure S1.

Synthesis of anhydrous sodium oxalate: Oxalic acid dihydrate (5 g, 39.7 mmol) was dissolved in 60 mL H_2O by stirring. NaOH (3.17 g, 79.3 mmol) was dissolved in 50 mL H_2O, and slowly added to the first solution while stirring. The resulting mixture was left to evaporate overnight at 80 °C, and then dried in an oven at 260 °C for five hours. Thermogravimetric analysis of the product (Figure S2) agrees with anhydrous sodium oxalate decomposition step at ca. 560 °C (exp. 21.0%, calc. 20.9%), yielding an equimolar amount of Na_2CO_3.[54] Diffuse reflectance FTIR spectroscopy: 3101, 3053, 2929, 2764, 2484, 1882, 1761, 1651, 1622, 1572, 1416, 1335, 1311, 1250, 771, 617, 517 cm^{-1}.

Synthesis of MIL-53: $AlCl_3{\cdot}6H_2O$ (966 mg, 4 mmol) was added to 30 mL demineralized H_2O inside a 45 mL Teflon liner. For modulated syntheses, 4 mmol of oxalic acid dihydrate was added (Table 1) and the solution was homogenized by stirring. Terephthalic acid (665 mg, 4 mmol) was added to the solution, and the mixture was stirred again (terephthalic acid is not completely dissolved in these conditions). The liner was sealed inside a steel autoclave and placed in an oven at 220 °C for 72 hours.

Synthesis of X-MIL-53 (X = CH_3O, OH, Br, NO_2): All reagent amounts and reaction temperatures are given in Table S1. A synthesis-specific amount of $AlCl_3{\cdot}6H_2O$ was added to 30 mL demineralized H_2O inside a 45 mL Teflon liner. Oxalic acid dihydrate was added in a specific stoichiometric amount and the solution was homogenized by stirring. An amount of linker in molar ratio 1:1 to $AlCl_3{\cdot}6H_2O$ was added and the solution was stirred again. The liner was sealed inside a steel autoclave and placed in an oven at a given temperature for 72 hours.

Table 1. Amount of modulator used for the syntheses of MIL-53.

Modulator	Amount
HCl 37%	0.33 mL
NH_4F anhydrous	148 mg
HF 40%	0.17 mL
$Na_2C_2O_4$ anhydrous	536 mg
$H_2C_2O_4{\cdot}2H_2O$	504 mg

Synthesis of CAU-10: Four different syntheses were performed using a general procedure adapted from the one reported by Reinsch et al.[50] by using different amounts of oxalic acid: 0 mmol, 0.6 mmol (53 mg), 1.2 mmol (105 mg), and 1.8 mmol (158 mg). The general procedure is reported as follows.

$Al_2(SO_4)_3{\cdot}18H_2O$ (802 mg, 1.2 mmol) was dissolved in 10 mL of a 1:4 DMF-H_2O mixture in a 45 mL Teflon liner. A certain stoichiometric amount of oxalic acid dihydrate was added and the solution was homogenized by stirring. Isophthalic acid (199 mg, 1.2 mmol) was added and the solution was stirred again. The liner was sealed inside a steel autoclave and placed in an oven at 135 °C for 24 hours.

Synthesis of MIL-69: Four different syntheses were performed using a general procedure adapted from the one reported by Loiseau et al.[51] by using different amounts of oxalic acid: 0 mmol, 1.75 mmol (221 mg), 3.5 mmol (441 mg), and 5.25 mmol (662 mg). The general procedure is reported as follows.

$Al(NO_3)_3{\cdot}9H_2O$ (1313 mg, 3.5 mmol) was added to 5 mL H_2O inside a 45 mL Teflon liner. A certain stoichiometric amount of oxalic acid dihydrate was added and the solution was homogenized by stirring. 2,6-Naphthalenedicarboxylic acid (378 mg, 1.75 mmol) and KOH (236 mg, 4.2 mmol) were added and the solution was stirred again (the linker is not completely dissolved in these conditions). The liner was sealed inside a steel autoclave and placed in an oven at 210 °C for 16 hours.

Synthesis of Al(OH)ndc: Four different syntheses were performed using a general procedure adapted from the one reported by Comotti et al.[52] by using different amounts of oxalic acid: 0 mmol, 0.5 mmol (63 mg), 1.0 mmol (126 mg) and 1.5 mmol (189 mg). The general procedure is reported as follows.

$Al(NO_3)_3{\cdot}9H_2O$ (375 mg, 1 mmol) was added to 10 mL H_2O inside a 45 mL Teflon liner. A certain stoichiometric amount of oxalic acid dihydrate was added and the solution was homogenized by stirring. 1,4-Naphthalenedicarboxylic acid (108 mg, 0.5 mmol) was added and the solution was stirred again (the linker is not completely dissolved in these conditions). The liner was sealed inside a steel autoclave and placed in an oven at 180 °C for 24 hours.

Post-synthesis treatment: After every MOF synthesis, the same treatment was applied to the products. The autoclave was cooled down slowly to room temperature and the solids were removed from the mother liquor by centrifugation. The products were subsequently rinsed three times: with 10 mL of DMF, with 10 mL demineralized water, and with 10 mL ethanol. The washed solids were placed in a glass vial and dried in a vacuum oven at 40 °C for 12 hours.

Analytical techniques: SEM analyses were performed using a JEOL JSM-6010LA InTouchScope scanning electron microscope. Morphological micrographs were obtained using a secondary electron detector and an acceleration voltage of 5 kV. X-ray microanalyses were obtained by energy-dispersive X-ray (EDX) spectra acquired with an acceleration voltage of 20 kV. All samples underwent a gold-coating preparation prior to the analysis. SEM images and EDX spectra were processed using the InTouchScope software Version 1.12.

Thermogravimetric analyses (TGA) were performed using a Mettler Toledo TGA/SDTA 851e under 100 mL min^{-1} air flow from 30 to 700 °C with a heating rate of 5 °C min^{-1}. The data were processed using the STARe SW 14.00 software.

Nitrogen adsorption/desorption isotherms were measured volumetrically in a Tristar II 3020 Micromeritics instrument at 77 K. The samples were activated by thermal treatment at 603 K for 72 h and degassed before the measurement at 433 K under N_2 flow for 16 h. The pore volume values were obtained from the data at $P/P_0 =$ 0.95.

X-ray powder diffractograms of the products were collected in Bragg–Brentano geometry using a Bruker-AXS D5005 equipped with a Co Kα source operating at 35 kV and 40 mA. Data collections were performed using a variable divergence slit and a step size of 0.02° in 2θ. Single-crystal XRD experiments on MIL-53 and NO_2-MIL-53 were performed at the XRD1 beamline of the Elettra Synchrotron facility (CNR Trieste, Basovizza, Italy).[55] Diffraction data were collected using a monochromatic 0.61 Å wavelength at 250 K (MIL-53) and 100 K (NO_2-MIL-53), using a cold nitrogen stream produced with an Oxford Cryostream 700 (Oxford Cryosystems Ltd., Oxford, United Kingdom). Diffraction datasets have been processed using the Rigaku CrysAlisPro version 1.171.38.43 software (Rigaku Corporation, Oxford, United Kingdom), which was also used for the reconstruction of the reciprocal space and precession images.

Acknowledgements

The Elettra Synchrotron facility (CNR Trieste, Basovizza, Italy) is acknowledged for granting beamtime at the single-crystal diffraction beamline XRD1 (Proposal ID 20185483) and the beamline staff is gratefully thanked for the precious assistance. This work was funded by the European Research Council (grant number 759212) within the Horizon 2020 Framework Programme (H2020-EU.1.1). The work by A.G.-N. forms part of the research programme of DPI, NEWPOL project 731.015.506.

Conflict of interest

The authors declare no conflict of interest.

Keywords: aluminium · chelates · crystal growth · metal-organic frameworks · modulated synthesis

[1] A. F. Masters, T. Maschmeyer, *Microporous Mesoporous Mater.* **2011**, *142*, 423 – 438.
[2] Z. Wang, J. Yu, R. Xu, *Chem. Soc. Rev.* **2012**, *41*, 1729 – 1741.
[3] W. Vermeiren, J.-P. Gilson, *Topics in Catalysis* **2009**, *52*, 1131 – 1161.
[4] Y. Ren, Z. Ma, P. G. Bruce, *Chem. Soc. Rev.* **2012**, *41*, 4909.
[5] S. Yuan, L. Feng, K. Wang, J. Pang, M. Bosch, C. Lollar, Y. Sun, J. Qin, X. Yang, P. Zhang, Q. Wang, L. Zou, Y. Zhang, L. Zhang, Y. Fang, J. Li, H.-C. Zhou, *Adv. Mater.* **2018**, *30*, 1704303.
[6] M. Sánchez-Sánchez, N. Getachew, K. Díaz, M. Díaz-García, Y. Chebude, I. Díaz, *Green Chem.* **2015**, *17*, 1500 – 1509.
[7] S. Biswas, T. Ahnfeldt, N. Stock, *Inorg. Chem.* **2011**, *50*, 9518 – 9526.
[8] S. Wang, C. Serre, *ACS Sustainable Chem. Eng.* **2019**, *7*, 11911 – 11927.
[9] T. Devic, C. Serre, *Chem. Soc. Rev.* **2014**, *43*, 6097 – 6115.
[10] J. J. Low, P. Jakubczak, J. F. Abrahamian, S. A. Faheem, R. R. Willis, A. I. Benin, J. J. Low, R. R. Willis, J. F. Abrahamian, P. Jakubczak, J. F. Abrahamian, S. A. Faheem, R. R. Willis, *J. Am. Chem. Soc.* **2009**, *131*, 15834 – 15842.
[11] N. Tannert, C. Jansen, S. Nießing, C. Janiak, *Dalton Trans.* **2019**, *48*, 2967 – 2976.
[12] F. Fathieh, M. J. Kalmutzki, E. A. Kapustin, P. J. Waller, J. Yang, O. M. Yaghi, *Sci. Adv.* **2018**, *4*, eaat3198.
[13] D. Lenzen, P. Bendix, H. Reinsch, D. Fröhlich, H. Kummer, M. Möllers, P. P. C. Hügenell, R. Gläser, S. Henninger, N. Stock, *Adv. Mater.* **2018**, *30*, 1705869.
[14] D. Lenzen, J. Zhao, S.-J. Ernst, M. Wahiduzzaman, A. Ken Inge, D. Fröhlich, H. Xu, H.-J. Bart, C. Janiak, S. Henninger, G. Maurin, X. Zou, N. Stock, *Nat. Commun.* **2019**, *10*, 3025.
[15] A. Permyakova, O. Skrylnyk, E. Courbon, M. Affram, S. Wang, U. H. Lee, A. H. Valekar, F. Nouar, G. Mouchaham, T. Devic, G. De Weireld, J. S. Chang, N. Steunou, M. Frère, C. Serre, *ChemSusChem* **2017**, *10*, 1419 – 1426.
[16] A. Samokhvalov, *Coord. Chem. Rev.* **2018**, *374*, 236 – 253.
[17] D. Feng, K. Wang, Z. Wei, Y.-P. Chen, C. M. Simon, R. K. Arvapally, R. L. Martin, M. Bosch, T.-F. Liu, S. Fordham, D. Yuan, M. A. Omary, M. Haranczyk, B. Smit, H.-C. Zhou, *Nat. Commun.* **2014**, *5*, 5723.
[18] F. Millange, R. I. Walton, *Isr. J. Chem.* **2018**, *58*, 1019 – 1035.
[19] O. K. Farha, A. M. Spokoyny, K. L. Mulfort, S. Galli, J. T. Hupp, C. A. Mirkin, *Small* **2009**, *5*, 1727 – 1731.
[20] H. J. Lee, J. We, J. O. Kim, D. Kim, W. Cha, E. Lee, J. Sohn, M. Oh, *Angew. Chem. Int. Ed.* **2015**, *54*, 10564 – 10568; *Angew. Chem.* **2015**, *127*, 10710 – 10714.
[21] S. Tanaka, K. Fujita, Y. Miyake, M. Miyamoto, Y. Hasegawa, T. Makino, S. Van Der Perre, J. Cousin Saint Remi, T. Van Assche, G. V. Baron, J. F. M. Denayer, *J. Phys. Chem. C* **2015**, *119*, 28430 – 28439.
[22] W. Cai, A. Gładysiak, M. Anioła, V. J. Smith, L. J. Barbour, A. Katrusiak, *J. Am. Chem. Soc.* **2015**, *137*, 9296 – 9301.
[23] S. Henke, W. Li, A. K. Cheetham, *Chem. Sci.* **2014**, *5*, 2392.
[24] K. J. Gagnon, C. M. Beavers, A. Clearfield, *J. Am. Chem. Soc.* **2013**, *135*, 1252 – 1255.
[25] E. A. Kapustin, S. Lee, A. S. Alshammari, O. M. Yaghi, *ACS Cent. Sci.* **2017**, *3*, 662 – 667.
[26] M. Mon, J. Ferrando-Soria, M. Verdaguer, C. Train, C. Paillard, B. Dkhil, C. Versace, R. Bruno, D. Armentano, E. Pardo, *J. Am. Chem. Soc.* **2017**, *139*, 8098 – 8101.
[27] S. M. Yoon, S. C. Warren, B. A. Grzybowski, *Angew. Chem. Int. Ed.* **2014**, *53*, 4437 – 4441; *Angew. Chem.* **2014**, *126*, 4526 – 4530.
[28] H. Bunzen, A. Javed, D. Klawinski, A. Lamp, M. Grzywa, A. Kalytta-Mewes, M. Tiemann, H.-A. K. von Nidda, T. Wagner, D. Volkmer, *ACS Appl. Nano Mater.* **2019**, *2*, 291 – 298.
[29] H. W. B. Teo, A. Chakraborty, S. Kayal, *Microporous Mesoporous Mater.* **2018**, *272*, 109 – 116.
[30] H. R. Abid, Z. H. Rada, X. Duan, H. Sun, S. Wang, *Energy Fuels* **2018**, *32*, 4502 – 4510.
[31] X. Wang, A. J. Jacobson, *J. Solid State Chem.* **2016**, *236*, 230 – 235.
[32] Y. Guo, J. Zhang, L.-Z. Dong, Y. Xu, W. Han, M. Fang, H.-K. Liu, Y. Wu, Y.-Q. Lan, *Chem. Eur. J.* **2017**, *23*, 15518 – 15528. Intensities attributable to impurities are visible in the XRD patterns of the products reported in the Supporting information file, Figure S4.
[33] M. Vougo-Zanda, J. Huang, E. Anokhina, X. Wang, A. J. Jacobson, *Inorg. Chem.* **2008**, *47*, 11535 – 11542.
[34] T. Loiseau, L. Lecroq, C. Volkringer, J. Marrot, G. Férey, M. Haouas, F. Taulelle, S. Bourrelly, P. L. Llewellyn, M. Latroche, *J. Am. Chem. Soc.* **2006**, *128*, 10223 – 10230.
[35] P. Caullet, J.-L. Paillaud, A. Simon-Masseron, M. Soulard, J. Patarin, *Comptes Rendus Chim.* **2005**, *8*, 245 – 266.
[36] J. B. Fein, J. E. Hestrin, *Geochim. Cosmochim. Acta* **1994**, *58*, 4817 – 4829.

[37] F. Thomas, A. Masion, J. Y. Bottero, J. Rouiller, F. Genevrier, D. Boudot, *Environ. Sci. Technol.* **1991**, *25*, 1553 – 1559.
[38] T. Loiseau, C. Serre, C. Huguenard, G. Fink, F. Taulelle, M. Henry, T. Bataille, G. Férey, *Chem. Eur. J.* **2004**, *10*, 1373 – 1382.
[39] C. Nanthamathee, S. Ling, B. Slater, M. P. Attfield, *Chem. Mater.* **2015**, *27*, 85 – 95.
[40] L. Liu, X. Wang, A. J. Jacobson, *Dalton Trans.* **2010**, *39*, 1722 – 1725.
[41] M. J. Cliffe, W. Wan, X. Zou, P. A. Chater, A. K. Kleppe, M. G. Tucker, H. Wilhelm, N. P. Funnell, F.-X. Coudert, A. L. Goodwin, *Nat. Commun.* **2014**, *5*, 4176.
[42] D. Balestri, I. Bassanetti, S. Canossa, C. Gazzurelli, A. Bacchi, S. Bracco, A. Comotti, P. Pelagatti, *Cryst. Growth Des.* **2018**, *18*, 6824 – 6832.
[43] C. R. Groom, I. J. Bruno, M. P. Lightfoot, S. C. Ward, *Acta Crystallogr. Sect. B* **2016**, *72*, 171 – 179.
[44] J. M. Moreno, A. Velty, J. A. Vidal-Moya, U. Díaz, A. Corma, *Dalton Trans.* **2018**, *47*, 5492 – 5502.
[45] J. M. Chin, E. Y. Chen, A. G. Menon, H. Y. Tan, A. T. S. Hor, M. K. Schreyer, J. Xu, *CrystEngComm* **2013**, *15*, 654 – 657.
[46] F. J. Carmona, C. R. Maldonado, S. Ikemura, C. C. Romão, Z. Huang, H. Xu, X. Zou, S. Kitagawa, S. Furukawa, E. Barea, *ACS Appl. Mater. Interfaces* **2018**, *10*, 31158 – 31167.
[47] G. Cai, H.-L. Jiang, *Angew. Chem. Int. Ed.* **2017**, *56*, 563 – 567; *Angew. Chem.* **2017**, *129*, 578 – 582.
[48] W. P. Ozimiński, J. C. Dobrowolski, *J. Phys. Org. Chem.* **2009**, *22*, 769 – 778.
[49] C. A. Hollingsworth, P. G. Seybold, C. M. Hadad, *Int. J. Quantum Chem.* **2002**, *90*, 1396 – 1403.
[50] H. Reinsch, M. A. van der Veen, B. Gil, B. Marszalek, T. Verbiest, D. de Vos, N. Stock, *Chem. Mater.* **2013**, *25*, 17 – 26.
[51] T. Loiseau, C. Mellot-Draznieks, H. Muguerra, G. Férey, M. Haouas, F. Taulelle, *Comptes Rendus Chim.* **2005**, *8*, 765 – 772.
[52] A. Comotti, S. Bracco, P. Sozzani, S. Horike, R. Matsuda, J. Chen, M. Takata, Y. Kubota, S. Kitagawa, *J. Am. Chem. Soc.* **2008**, *130*, 13664 – 13672.
[53] K. Otake, M. Matsumoto, S. Tanaka, S. Uchida, R. Goseki, A. Hirao, T. Ishizone, *Macromol. Chem. Phys.* **2017**, *218*, 1600550.
[54] K. Suba, M. R. Udupa, *J. Therm. Anal.* **1989**, *35*, 1197 – 1203.
[55] A. Lausi, M. Polentarutti, S. Onesti, J. R. Plaisier, E. Busetto, G. Bais, L. Barba, A. Cassetta, G. Campi, D. Lamba, A. Pifferi, S. C. Mande, D. D. Sarma, S. M. Sharma, G. Paolucci, *Eur. Phys. J. Plus* **2015**, *130*, 43.

Manuscript received: October 21, 2019
Revised manuscript received: December 19, 2019
Accepted manuscript online: January 8, 2020
Version of record online: March 3, 2020

